On Evaporation of a Thin-Film Coated on a Substrate

S.E.-S. Abd El-Ghany [*] ***and A.F.Hassan*** [**]

[*]Department of physics, Faculty of Science, Benha University, Benha, Egypt
[**]Department of physics, Faculty of Science, Helwan University, Cairo, Egypt

The two-dimensional Laplace integral transform technique has been applied to get the spatial and temporal temperature distributions in both the molten layer thickness of a thin film coated on a substrate, the still solid part of the thin film of the target and the temperature distribution in the substrate. Also a formula for the time dependence of the evaporated part and the molten layer thickness of the thin-film as a function of time were obtained. The derivation has taken into account the temperature dependent absorption coefficient of the irradiated surface and the chemical reaction in the vapor of the thin film. Calculations of the obtained relations were carried out during the irradiation of aluminum thin film coated on a glass substrate with a pulsed laser.

1. Introduction:

The very high power density of some types of lasers used in material processing [1-3] and material science [4] might lead to damage the laser materials and/ or, the components necessary for the lasing process and its confinement. Therefore, an understanding of the mechanisms which cause radiation damage in optical components and the materials employed in a laser are of great importance.

Several authors have considered different aspects in treating these problems [5-16]. El-Nicklawy et al. [17] have studied the problem of melting a semi-infinite target irradiated with a pulsed laser assuming the temperature distribution in the molten layer to be constant and equal to the melting temperature (T_m). Abd El-Ghany [18] has studied the same problem considering a temperature profile in the molten layer. Abd El-Ghany [19] also studied the problem of melting with temperature profile in the molten layer of a thin-film coated on a substrate induced by irradiation with a pulsed laser. He calculated the molten layer thickness as a function of time as well as the temperature

distribution inside the liquid, the still solid part of the film and in the substrate. Nevertheless the quantitative analysis of such problems still needs further trial at different conditions to obtain formula that can easily be computed in practical sense.

The present study aims to solve the problem of evaporation of a thin film coated on a substrate, induced by surface absorption of a time dependent laser pulse profile [5]. Mathematical expressions for the temperature distributions in both the liquid part, the still solid part of the thin film and in the substrate as well as the time dependence of the evaporated thickness of the thin film for different pulse durations and power were obtained. Calculations of the obtained relations were carried out for two cases, when no chemical reaction (case A) and when chemical reaction (case B) in the vapor is taken into consideration. Table (1) shows the symbols of the physical parameters, their definitions and units used in the calculations.

Table (1): Symbols, units and definitions of the physical parameters.

Symbol	Units	Definition
t_{ll}	s	Time measured after initiating the melting process
α_1	$m\ s^{-2}$	Thermal diffusivity of the liquid
t_m	s	Time of initiating the melting process
q_0	Wm^{-2}	Maximum laser power density
A_0		Temperature independent part of the surface absorption coefficient
s	s^{-1}	Temporal angular frequency
p	m^{-1}	Spatial angular frequency
A_{01}	K^{-1}	Temperature dependent part of the surface absorption coefficient
R	---	Given values zero or 1 depends upon the considered case A or B
ρ_{su}	$kg\ m^{-3}$	Density of the substrate of the target
cp_{su}	$J\ kg^{-1}\ K^{-1}$	Specific heat by constant pressure of the substrate
q_{ch}	$J\ kg^{-1}$	Latent heat of the considered chemical reaction
q_{ev}	$J\ kg^{-1}$	Latent heat of evaporation the thin-film
k_l	$Wm^{-1}\ K^{-1}$	Thermal conductivity of the liquid part of the thin-film
k_s	$Wm^{-1}\ K^{-1}$	Thermal conductivity of the solid part of the thin-film
ρ_l	$kg\ m^{-3}$	Density of the liquid part of the thin-film
ρ_s	$kg\ m^{-3}$	Density of the solid part of the thin-film
q_l	$J\ kg^{-1}$	Latent heat of melting the thin-film
α_s	$m\ s^{-2}$	Thermal diffusivity of the solid part of the thin-film
α_{su}	$m\ s^{-2}$	Thermal diffusivity of the substrate
cp_l	$J\ kg^{-1}\ K^{-1}$	Specific heat by constant pressure of the thin-film
T_m	K	Melting temperature of the thin-film
δt	s	Pulse duration
Tevl	K	Boiling temperature of the thin-film
L	m	Thickness of the thin-film

2. Theory:

Assuming a laser pulse of arbitrary relative temporal intensity distribution g(t) to be incident perpendicular to a thin-film coated on a substrate as a target. Since the laser pulse possesses enough energy to initiate melting and evaporation processes, it will be subdivided into three parts: the first part is responsible for the heating process up to the time of reaching the front surface of the thin-film the melting temperature [19]. The second part deals with the time responsible for the molten layer to reach the evaporation temperature [19].The third part, which is the subject of this paper, is responsible for the evaporation process. The study

Includes two different cases:

A) No chemical reaction in the vapor was assumed.
B) Chemical reaction in the vapor was considered.

The temperature dependence of the material parameters except the absorption coefficient, which is assumed to be linearly dependent on the surface temperature during all the considered processes (heating, melting and evaporation), as well as non-linear effects such as multi-photons absorption and plasma formation in front of the irradiated surface were neglected. The relations governing the temperature distributions within the liquid, the solid part of the thin-film and the substrate as well as the evaporated thickness of the thin-film as a function of time are given for one dimensional problem by the following equations:

1) The heat diffusion equation in the liquid part of the thin-film

$$\frac{\partial^2 T_1(x_{l_1}, t_{ev})}{\partial x_{l_1}^{\ 2}} - \frac{1}{\alpha_1}\frac{\partial T_1(x_{l_1}, t_{ev})}{\partial t_{ev}} = 0 \quad \textbf{valid for } x_{l_1} \le x_1(t_{ev}) \qquad (1)$$

where $T_1(x_{l_1}, t_{ev})$ is the excess temperature distribution above ambient in the liquid part of the thin-film, x_{l_1} the spatial coordinate in the liquid with origin at the front surface of the liquid and $x_1(t_{ev})$ is the molten layer thickness of the liquid and t_{ev} is the time measured after initiating of the evaporation process.

2) The differential heat balance equation at the front surface of the liquid

$$q_{l0}g(t_{ev}+t_{ll}+t_m)[A_0+A_{01}Tev]+R\rho_1 q_{ch}\dot{x}_{ev}(t_{ev}) = -k_1\left.\frac{\partial T_1(x_{l_1}, t_{ev})}{\partial x_{l_1}}\right|_{x_{l_1}=0} + \rho_1 q_{ev}\dot{x}_{ev}(t_{ev}) \quad (2)$$

where $g(t_{ev}+ t_{ll}+t_m)$ is the relative temporal intensity distribution of the laser pulse profile with maximum value one and $\dot{x}_{ev}(t_{ev})$ is the rate of change of the evaporated thickness of the thin-film.

3) The heat diffusion equation in the solid part of the thin-film

$$\frac{\partial^2 T_s(x_s, t_{ev})}{\partial x_s^{\,2}} - \frac{1}{\alpha_s}\frac{\partial T_s(x_s, t_{ev})}{\partial t_{ev}} = 0 \qquad (3)$$

where $T_s(x_s, t_{ev})$ is the excess temperature distribution above ambient in the solid part of the thin-film, x_s is the spatial coordinate of the solid part with origin at the liquid /solid interface.

4) The boundary condition at the vapor-liquid interface of the thin-film

$$T_l(0, t_{ev}) = \mathbf{Tevl} \qquad (4)$$

where $T_l(0, t_{ev})$ is the excess temperature distribution above ambient at the surface of the liquid thickness.

5) The boundary condition at the liquid-solid interface of the thin-film

$$T_l(x_{l_1}, t_{ev})_{x_{l_1}=x_l} = T_s(x_s, t_{ev})_{x_s=0} = T_m \qquad (5)$$

where $T_s(0, t_{ev})$ is the excess temperature distribution above ambient at the surface of the still solid part of the thin-film.

6) The boundary condition at the solid - substrate interface

$$T_s(x_s, t_{ev})_{x_s = L-(x_l(t_{ev})+x_{ev}(t_{ev}))} = T_{su}(x_{su}, t_{ev})_{x_{su}=0} \qquad (6)$$

7) The heat diffusion equation in the substrate of the target

$$\frac{\partial^2 T_{su}(x_{su}, t_{ev})}{\partial x_{su}^{\,2}} - \frac{1}{\alpha_{su}}\frac{\partial T_{su}(x_{su}, t_{ev})}{\partial t_{ev}} = 0 \qquad (7)$$

where $T_{su}(x_{su}, t_{ev})$ is the excess temperature distribution above ambient in the substrate, x_{su} is the spatial coordinate of the substrate with origin at the solid-substrate interface.

8) The tendency of vanishing the temperature in the substrate as $x_{su} \to \infty$

$$\lim_{x_{su}\to\infty} T_{su}(x_{su}, t_{ev}) = 0. \tag{8}$$

9) The integrated heat balance equation

$$\int_0^{t_m}[A_0 + A_{01}T(0,t)]q_0 g(t)dt + \int_{t_m}^{t_{ev}}[A_0 + A_{01}T_m]q_0 g(t)dt + \int_{t_{ev}}^{\delta t}[A_0 + A_{01}Tevl]q_0 g(t)dt +$$

$$R\int_{t_{ev}}^{\delta t}\rho_l q_{ch}\dot{x}_{ev}(t)dt = \int_{t_m}^{t_{ev}}\rho_l q_l \dot{x}_l(t)dt + \int_{t_{ev}}^{\delta t}\rho_l q_{ev}\dot{x}_{ev}(t)dt + \int_0^{x_l(t_{ev})}\rho_l cp_l T_l(x_{l_1}, t_{ev})dx_{l_1} +$$

$$\int_0^{x_s(t_{ev})}\rho_s cp_s T_s(x_s, t_{ev})dx_s + \int_0^{\infty}\rho_{su} cp_{su} T_{su}(x_{su}, t_{ev})dx_{su} + \rho_l cp_l Tevl.x_{ev}(t_{ev}) \tag{9}$$

where: T(0,t) is the excess surface temperature above ambient of the film up to initiating the melting process and $\dot{x}_l(t)$ is the rate of change of the molten layer thickness.

The two dimensional integral Laplace transform technique is applied on the above cited equations requires the knowledge of the temperature distribution within both the liquid part and the still solid part of the thin-film and in the substrate at the time of initiating the melting process and at the time of initiating the evaporation process [19]. This technique leads to an algebraic relations in s and p domain when applied on the equations (1) considering equation (4). The inverse Laplace transform w.r.t. the complex spatial angular frequency p, gives the temperature distribution in the molten layer of the thin-film $\tilde{T}_1(x_{l_1}, s)$ as a function of the complex temporal angular frequency s as:

$$\tilde{T}_1(x_{l_1}, s) = \frac{Tevl}{s}\cosh(\sqrt{s/\alpha_l})x_{l_1} - T_{lb.ev}(x_0, t_l)\left[\frac{\cosh(\sqrt{s/\alpha_l})x_{l_1} - 1}{s}\right] +$$

$$\left.\frac{\partial\tilde{T}_l(x_{l_1}, s)}{\partial x_{l_1}}\right|_{x_{l_1}=0}\frac{\sinh(\sqrt{s/\alpha_l})x_{l_1}}{\sqrt{s/\alpha_l}} \tag{10}$$

صhere $T_{lb.ev}(x_0, t_l)$ is the temperature distribution in the liquid part of the thin-film just at the moment of initiating the evaporation process. It is given according to [19] when the cooling is neglected by the following equation;

$$T_{lb.ev}(x_0, t_l) = \frac{\sqrt{\alpha_1}}{k_1}\int_0^{t_l} G_1(\tau + t_m)\left[\frac{\exp(-(x_0{}^2/4\alpha_1(t_l-\tau)))}{\sqrt{\pi(t_l-\tau)}}\right]d\tau + T_{1b.m}(x,t) \qquad (11)$$

where: $G_1(\tau+t_m)= q_0 g(\tau+t_m)[A_0+A_{01}\, T_l(0, \tau)]$

$T_l(0, \tau)$ is the time dependent surface temperature during the melting process, τ is the time between 0 and t_{ll} , $t_1= t_{ll}+t_{ev}$, $x_0=x_{ev}+x_l$ and $T_{lb.m}(x,t)$ is the temperature distribution within the thin-film as the surface temperature has reached the melting temperature (T_m). It is given when the cooling is neglected, according to [19] by:

$$T_{1b\cdot m}(x,t) = \frac{q_o G(t)}{2} * \left(2C_1 \frac{\exp(-x^{\,2}/(4\alpha_2 t))}{(\pi t)^{1/2}} + \right.$$

$$\left. + \sum_{i=1}^{2}\sum_{j=1}^{2}\left(a_{ij}\frac{\exp\left(-(2iL + (-1)^j x)^2/(4\alpha_2 t)\right)}{(\pi t)^{1/2}}\right)\right) \qquad (12)$$

where * is sign for convolution w.r.t. the time.
With

$$G(\tau) = g(\tau).[A_o + A_{01}T(0,\tau)]\ ;\ M_1 = \frac{\rho_2 cp_2\sqrt{\alpha_3}}{\rho_1 cp_1\sqrt{\alpha_2}}\ \ ;\ \ M_2 = \rho_2 cp_2\sqrt{\alpha_3} + \rho_1 cp_1\sqrt{\alpha_2};$$

$$M_4 = \rho_1 cp_1\sqrt{\alpha_2}\ ; M_5 = \rho_2 cp_2\sqrt{\alpha_3}\ ; M_7 = M_5 - M_4\ ; C_1 = \frac{1+M_1}{M_2}\ ;\ \ C_3 = \frac{1-M_1}{M_2};$$

$a_{11}=2C_3$; $a_{12}=2C_3$; $a_{21}=-C_3M_7/M_2$ and $a_{22}=a_{21.}$

$T(0, \tau)$ is the time dependent surface temperature during the heating process, τ is the time between 0 and t_m and $t= t_l+t_m$, $x=x_{ev}+x_l$ in liquid and $x=x_{ev}+x_l+x_s$ in solid part of the thin-film, $\alpha_2= \alpha_s$, $\alpha_3= \alpha_{su}$, $\rho_1= \rho_s$, $\rho_2= \rho_{su}$,$cp_1=cp_s$ and $cp_2=cp_{su}$.

Applying the initial value theorem given by

$$\lim_{s\to\infty} s\tilde{T}_1(x_{l_1},s) = \lim_{t_{ev}\to 0} T_{lb\cdot ev}(x_0,t_l)$$

on eqn.(10), one gets $$\left.\frac{\partial \tilde{T}_l(x_{l_1},s)}{\partial x_{l_1}}\right|_{x_{l_1}=0} = \frac{T_{lb.ev}(x_0,t_1) - Tevl}{\sqrt{s\alpha_l}}. \qquad (13)$$

Substituting from equation (13) into eqn. (10) and using the inverse Laplace transform technique w.r.t. s, one gets

$$T_l(x_{l_1},t_{ev}) = Tevl.Erfc\left(\frac{x_{l_1}}{2\sqrt{t_{ev}\alpha_l}}\right) + T_{lb.ev}(x_0,t_l)\left[1 - Erfc\left(\frac{x_{l_1}}{2\sqrt{t_{ev}\alpha_l}}\right)\right] \qquad (14)$$

Applying the Laplace transform technique on eqn.(3) considering eqn.(5) gives the temperature distribution in the solid part of the thin-film $\tilde{\tilde{T}}_s(p,s)$ in p and s domain. The inverse Laplace transform w.r.t. the complex spatial angular frequency p, gives the temperature distribution in the still solid part of the thin-film $\tilde{T}_s(x_s,s)$ as:

$$\tilde{T}_s(x_s,s) = \frac{T_m}{s}\cosh(\sqrt{s/\alpha_s})x_s - T_{sb.ev}(\eta_0,t_l)\left[\frac{\cosh(\sqrt{s/\alpha_s})x_s - 1}{s}\right] +$$

$$\left.\frac{\partial \tilde{T}_s(x_s,s)}{\partial x_s}\right|_{x_s=0} \frac{\sinh(\sqrt{s/\alpha_s})x_s}{\sqrt{s/\alpha_s}} \qquad (15)$$

$T_{sb.ev}(\eta_0,t_l)$ is the temperature distribution in the solid part of the thin-film just at the time of initiating the evaporation process. It is given according to [19] by the following equation:

$$T_{sb.ev}(\eta_0,t_l) = T_m Erfc\left(\frac{\eta_0}{2\sqrt{t_l\alpha_2}}\right) + T_{1b.m}(x,t)\left[1 - Erfc\left(\frac{\eta_0}{2\sqrt{t_l\alpha_2}}\right)\right]$$

where: $t_l = t_{ll} + t_{ev}$; $t = t_l + t_m$; $x_s = \eta_0$ and $x = x_{ev} + x_l + x_s$.

Applying the initial value theorem given by

$$\lim_{s\to\infty} s\tilde{T}_s(x_s,s) = \lim_{t_{ev}\to 0} T_{sb.ev}(\eta_0,t_l)$$

on eq.(15), the value of $\left.\frac{\partial \tilde{T}_s(x_s,s)}{\partial x_s}\right|_{x_s=0}$, after setting the sum of the coefficients of $\exp(\sqrt{s/\alpha_2}\, x_s)$ equal to zero, can be obtained. Substituting the obtained expression for $\left.\frac{\partial \tilde{T}_s(x_s,s)}{\partial x_s}\right|_{x_s=0}$ into eq.(15) and using the inverse Laplace transform technique w.r.t. s one gets:

$$T_s(x_s,t_{ev}) = T_m \operatorname{Erfc}\left(\frac{x_s}{2\sqrt{t_{ev}\alpha_s}}\right) + T_{sb.ev}(\eta_0,t_l)\left[1-\operatorname{Erfc}\left(\frac{x_s}{2\sqrt{t_{ev}\alpha_s}}\right)\right] \quad (16)$$

Eq.(16) gives the temperature distribution within the still solid part of the thin-film of the target.

Applying the Laplace transform technique on equation (7), the temperature distribution in the substrate of the target in p and s domain can be given by:

$$\tilde{\tilde{T}}_{su}(p,s) = \frac{p\,\tilde{T}_{su}(0,s)}{p^2-\frac{s}{\alpha_{su}}} - \frac{\tilde{T}_{su.b.ev}(p,t_l)}{\alpha_{su}(p^2-\frac{s}{\alpha_{su}})} + \frac{1}{(p^2-\frac{s}{\alpha_{su}})}\left.\frac{\partial \tilde{T}_{su}(x_{su},s)}{\partial x_{su}}\right|_{x_{su}=0}$$

Using the inverse Laplace transform technique w.r.t. p on the above equation, $\tilde{T}_{su}(x_{su},s)$ can be obtained as:

$$\tilde{T}_{su}(x_{su},s) = \tilde{T}_{su}(0,s)\cosh(\sqrt{s/\alpha_{su}})x_{su} + \left.\frac{\partial \tilde{T}_{su}(x_{su},s)}{\partial x_{su}}\right|_{x_{su}=0}\frac{\sinh(\sqrt{s/\alpha_{su}})x_{su}}{\sqrt{s/\alpha_{su}}} - \frac{1}{\alpha_{su}}\int_0^{x_{su}}\frac{T_{su.b.ev}(\zeta,t_l)}{\sqrt{s/\alpha_{su}}}\sinh\left(\sqrt{s/\alpha_{su}}(x_{su}-\zeta)\right)d\zeta \quad (17)$$

where $T_{su.b.ev}(\zeta,t_l)$ is the temperature distribution in the substrate at the time of initiating the evaporation process. It is given according to [19] by the following equation:

$$T_{su.b.ev}(\zeta,t_l) = T_m \operatorname{Erfc}\left[\frac{L-sx(t_l)+\frac{\zeta}{\sqrt{\alpha_3}}}{2\sqrt{t_l}}\right] - T_{1b.m}(L,t)\operatorname{Erfc}\left[\frac{\frac{L-sx(t_l)}{\sqrt{\alpha_2}}+\frac{\zeta}{\sqrt{\alpha_3}}}{2\sqrt{t_l}}\right] + T_{1b.m}(L,t).$$

$$\mathrm{Erfc}\left(\frac{\zeta}{2\sqrt{\alpha_3 t_1}}\right)+\frac{1}{2\sqrt{\pi\alpha_3 t_1}}\int_0^{\infty} T_{su.b.m}(\zeta_1,t)\left[\exp\left(-\left(\frac{(\zeta-\zeta_1)^2}{4\alpha_3 t_1}\right)\right)-\exp\left(-\left(\frac{(\zeta+\zeta_1)^2}{4\alpha_3 t_1}\right)\right)\right]d\zeta_1$$

where: $t_l=t_{ll}+t_{ev}$; $sx(t_1)=x_{ev}+x_l$; $t=t_m+t_l$; $\zeta=x_{su}$ and $T_{su.b.m}(\zeta_1,t)$ is the temperature distribution in the substrate during the heating process which is given according to [19], when the cooling effect is neglected as:

$$T_{su.b.m}(\zeta_1,t)=\frac{q_o G(t)}{2}*\left[\sum_{i=1}^{3} d_i \frac{\exp\left[-\frac{\left((2i-1).(L/\sqrt{\alpha_2})+\zeta_1/\sqrt{\alpha_3}\right)^2}{4t}\right]}{(\pi t)^{1/2}}\right] \quad (18)$$

with: $d_1=2(C_1+C_3)$; $d_2=(C_3-(C_1+C_3)(M7/M_2))$ and $d_3=-\frac{C_3 M_7}{M_2}$.

$\tilde{T}_{su}(0,s)$ can be obtained by applying the Laplace transform on the boundary condition of equation (6). Substituting the value of $\tilde{T}_{su}(0,s)$ into equation (17) and using the boundary condition given by eqn. (8) which leads to set the sum of the coefficients of $\exp(\sqrt{s/\alpha_{su}}\,x_{su})$ equal to zero, gives the value of $\left.\frac{\partial\tilde{T}_{su}(x_{su},s)}{\partial x_{su}}\right|_{x_{su}=0}$. Substituting the value of $\left.\frac{\partial\tilde{T}_{su}(x_{su},s)}{\partial x_{su}}\right|_{x_{su}=0}$ into equation (17) and using the inverse of Laplace transform w.r.t. s, one gets:

$$T_{su}(x_{su},t_{ev})=T_m\mathrm{Erfc}\left[\frac{\frac{L-sx(t_{ev})}{\sqrt{\alpha_s}}+\frac{x_{su}}{\sqrt{\alpha_{su}}}}{2\sqrt{t_{ev}}}\right]-T_{s.b.ev}(L-sx(t_{ev}),t_l).\mathrm{Erfc}\left[\frac{\frac{L-sx(t_{ev})}{\sqrt{\alpha_s}}+\frac{x_{su}}{\sqrt{\alpha_{su}}}}{2\sqrt{t_{ev}}}\right]+$$

$$T_{s.b.ev}(L-sx(t_{ev}),t_l).\mathrm{Erfc}\left(\frac{x_{su}}{2\sqrt{\alpha_{su}t_{ev}}}\right)+ \quad (19)$$

$$\frac{1}{2\sqrt{\pi\alpha_{su}t_{ev}}}\int_0^{\infty} T_{su.b.ev}(\zeta_1,t)\left[\exp\left(-\left(\frac{(x_{su}-\zeta_1)^2}{4\alpha_{su}t_{ev}}\right)\right)-\exp\left(-\left(\frac{(x_{su}+\zeta_1)^2}{4\alpha_{su}t_{ev}}\right)\right)\right]d\zeta_1$$

Differentiating equation (14) w.r.t. x_{l_1} and substituting the obtained result into equation (2) after setting x_{l_1} equal to zero, the rate of change the evaporated thickness $\dot{x}_{ev}(t_{ev})$ can be calculated. Integrating $\dot{x}_{ev}(t_{ev})$ w.r.t. t_{ev} , gives:

$$x_{ev}(t_{ev}) = 2\lambda_l\left[\frac{-Tevl}{\rho_l[q_{ev}-Rq_{ch}]}\right]\sqrt{\frac{t_{ev}}{\pi\alpha_l}} + \frac{\lambda_l}{\rho_l[q_{ev}-Rq_{ch}]\sqrt{\pi\alpha_l}}\int_0^{t_{ev}}\frac{T_{lb.ev}(x_{ev}(t_{ev}),t_l)}{\sqrt{t_{ev}}}dt_{ev} +$$

$$\frac{q_0[A_0+A_{01}Tevl]}{\rho_l[q_{ev}-Rq_{ch}]}.\int_0^{t_{ev}} g(t_{ll}+t_m+\tau)d\tau \qquad (20)$$

To obtain $x_{ev}(t_{ev})$ from eq.(20) the Newton iteration method was applied. Substituting the x_{ev} values as a function of t_{ev} in eqn. (14) and using the condition of eqn.(5), the molten layer thickness x_l can be obtained as a function of t_{ev}.

3. Computations:

Equations (14,16,19,20) for the cases when R=0 and R=1 have been calculated for an aluminum thin-film coated on a glass substrate subjected to a relative distribution of the Ready pulse profile [5] approximated by the following relation [16].

$$g(t) = \begin{cases} \frac{(n+1)^{n+1}}{n^n}.\frac{t}{\delta t}.(1-\frac{t}{\delta t})^n & \text{for} \quad 0 \le t \le \delta t \\ 0 & \text{for} \quad t \ge \delta t \end{cases} \qquad (21)$$

where n is given the value 3. The physical and thermal parameters for aluminum and glass are shown in table (2) [20].

Table (2): The optical and thermal parameters of aluminum and glass

Element	$\underline{K}$ $Wm^{-1}K^{-1}$	ρ kg/m^3	cp J/kg.K	A_0	A_{01} K^{-1}
Al	238	2707	896	0.056	3.05×0^{-5}
Glass	17	$4.5x10^3$	1100		

Table (2): The optical and thermal parameters of aluminum (continued).

Element	q_l J/kg	q_{ev} J/kg	q_{ch} J/kg	T_m K	Tevl K
Al	4×10^5	1.08×10^7	1.671×10^7	633	2440

3.1. Case when no chemical reaction in the vapor (R=0) was considered:

Figure (1) represents, considering the values given in tables (3,4), the time dependence of the evaporated thicknesses of the thin-film (curves 1-6) and the normal temporal intensity distribution curve (7) when δt is kept constant at 2×10^{-6} s. The figure shows that the greatest values of q_0 and A_{01} leads to the greatest evaporation and that the evaporation at the end of the pulse duration decreases. This behavior can be explained in view of the fact that the greatest q_0 and A_{01} leads to the greatest absorbed energy and therefore the greatest value of x_{ev}. At the end of the laser pulse the evaporated thickness for the case A_{01} $=3.05\times10^{-5}$ K^{-1} (increased absorption) is about 3 times greater than that for $A_{01}=0$ K^{-1}.

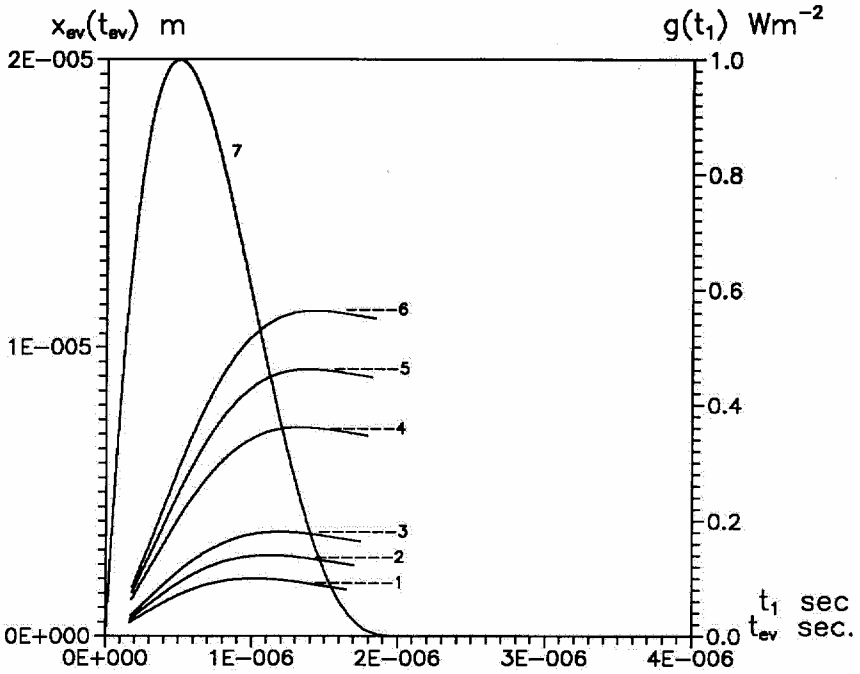

Fig.(1): The time dependence of the evaporated thickness $x_{ev}(t_{ev})$ calculated during the irradiation of an Al thin-film coated on a glass substrate with the Ready pulse profile $g(t_1)$ curve (7). The calculations were carried out considering R=0 and $\delta t = 2\times10^{-6}$ s for the cases listed in tables (3,4).

Table (3): The values of the melting time t_m, the time of initiating the evaporation process t_{ll} calculated for different q_0 values, $\delta t = 2\times10^{-6}$ s; $A_{01}=0$ K^{-1} and $L= 4\times10^{-5}$ m.

q_0 Wm^{-2}	t_m s	t_{ll} s	Curve no
2.5×10^{12}	1.2100×10^{-7}	2.2950×10^{-7}	1
3.0×10^{12}	1.0600×10^{-7}	1.9000×10^{-7}	2
3.5×10^{12}	9.4080×10^{-8}	1.6545×10^{-7}	3

Table (4): The values of the melting time t_m, the time of initiating the evaporation process t_{ll} calculated for different q_0 values, $\delta t = 2\times10^{-6}$ s; $A_{01}=3.05\times10^{-5}$ K^{-1} and $L= 4\times10^{-5}$ m for different q_0 values.

q_0 Wm^{-2}	t_m s	t_{ll} s	curve no
2.5×10^{12}	1.0350×10^{-7}	1.0776×10^{-7}	4
3.0×10^{12}	9.0800×10^{-8}	9.2050×10^{-8}	5
3.5×10^{12}	8.0870×10^{-8}	7.8460×10^{-8}	6

The first term in eq.(20), which represents liquidifcation will be more significant due to the small rate of increase of the other two terms. This fact leads to the observed decrease of x_{ev}.

Figure (2) represents for the same conditions cited previously in Fig.(1), the dependence of the molten layer thickness on the time measured from initiating the evaporation process up to the end of the laser pulse duration. The figure shows that the molten layer thickness increases with increasing the time. The figure shows also that for great q_0 and $A_{01}=3.05\times10^{-5}$ K^{-1}, the molten layer thickness is smaller than that for small q_0 and $A_{01}=0$ K^{-1}. This behavior can be attributed to the fact that for great values of q_0 and A_{01}, the energy consumed in the evaporating process is greater than the case of small q_0 and A_{01} values. This leads in-turn to decrease the energy required for the melting process.

Considering the conditions given in Fig.(1), Figs.(3,4) represent the temperature distribution within the molten layer thickness for the times $t_{ev}=\left[\frac{\delta t-(t_m+t_{ll})}{10}\right]$ and $t_{ev}=[\delta t-(t_m+t_{ll})]$ after initiating the evaporation process respectively. The figures show that the penetration depth increases with increasing the time, and that the penetration depth for the great q_0 value and A_{01} $=3.05\times10^{-5}$ $K^{-1}$is smaller than that for small q_0 and $A_{01}=0$ K^{-1}. This behavior can be attributed to the fact that, as seen from fig.(2), the molten layer thickness in case of $A_{01}=0$ K^{-1} and $q_0= 2.5\times10^{12}$ Wm^{-2} is greater than that for A_{01} $=3.05\times10^{-5}$ K^{-1} and $q_0= 3.5\times10^{12}$ Wm^{-2} .

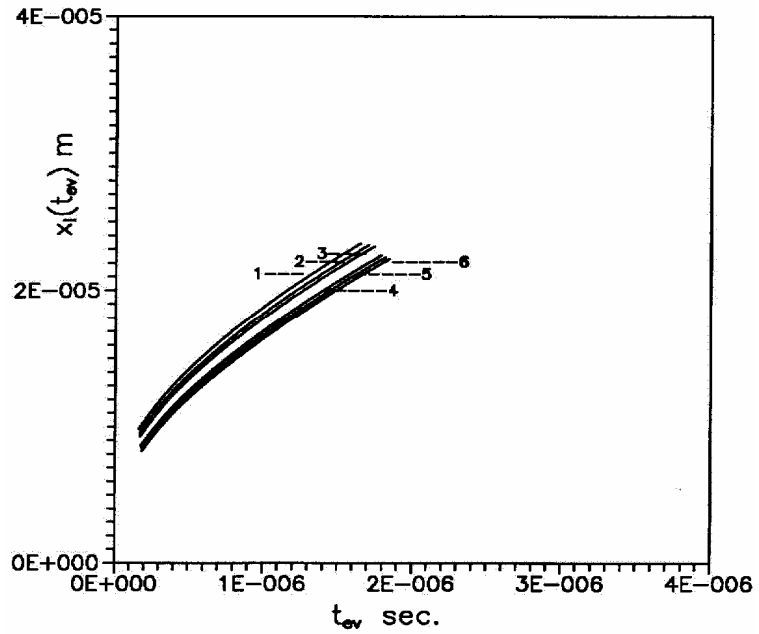

Fig.(2): The time dependence of $x_l(t_{ev})$ calculated during the irradiation of an Al thin-film coated on a glass substrate with the Ready pulse profile. The calculations were carried out considering R=0 and $\delta t = 2\times10^{-6}$ s for the cases listed in tables (3,4).

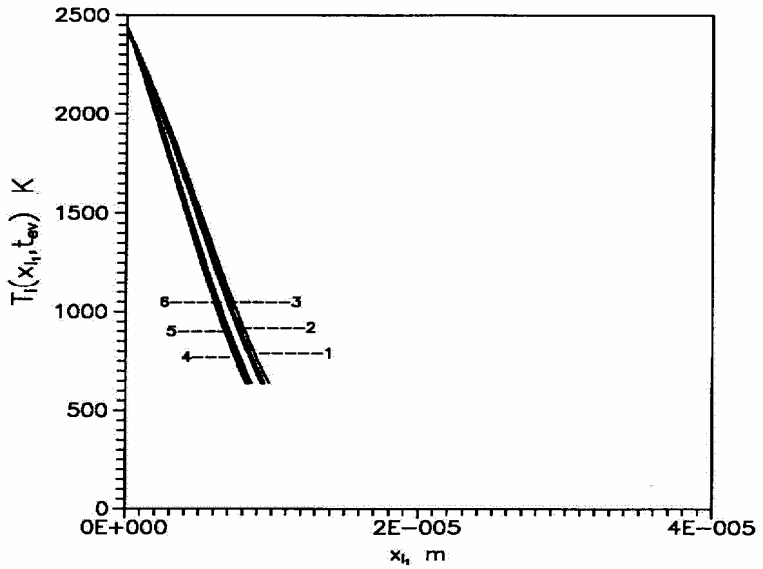

Fig.(3): The temperature distribution in the liquid part of an Al thin-film coated on a glass substrate, irradiated with a Ready pulse profile of $\delta t = 2\times10^{-6}$ s. The calculations were carried out for the cases listed in tables (3,4) at $t_{ev} = \left(\frac{\delta t - (t_m + t_{ll})}{10}\right)$ s after initiating the evaporation process and R=0.

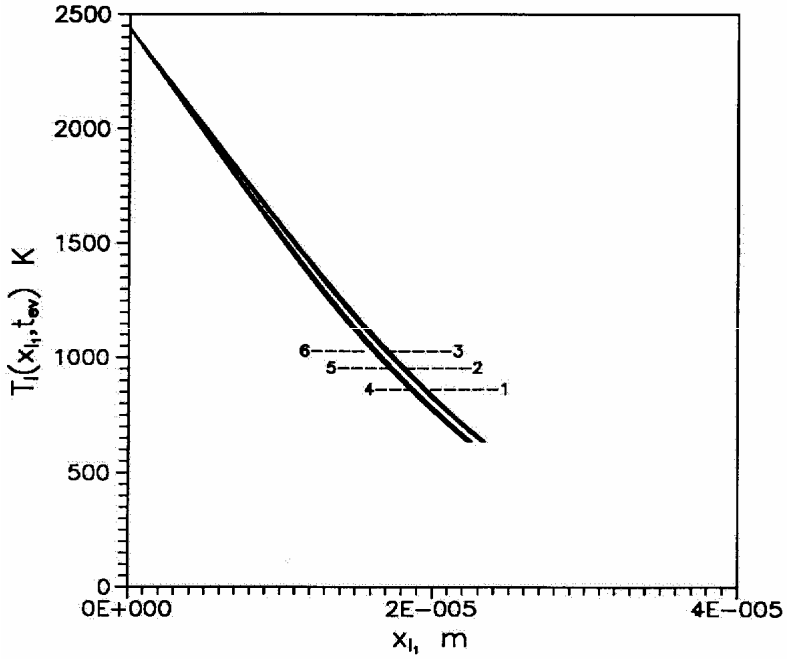

Fig.(4): The temperature distribution in the liquid part of an Al thin-film coated on a glass substrate, irradiated with a Ready pulse profile of $\delta t = 2\times10^{-6}$ s. The calculations were carried out for the cases listed in tables (3,4) at $t_{ev} = [\delta t - (t_m + t_{ll})]$ s after initiating the evaporation process and R=0.

Fig.(5) illustrates the temperature distributions within the solid part of the thin-film calculated at time $t_{ev} = \left[\frac{\delta t - (t_m + t_{ll})}{10}\right]$ considering the same conditions given in fig.(1). From the figure it is evident that curve (1) which correspond to the smallest absorbed energy has the highest temperature distribution. This behavior can be attributed to the fact that, the time at which curve (1) was calculated is the greatest when measuring the time from initiating the laser pulse. Due to the greatest melting and evaporation time, the evaporated thickness in this case is the smallest. In spite of these facts most of the absorbed energy was consumed in the heating process leading to the highest temperature distribution and penetration.

The calculated heat balance equation (9), at the end of the laser pulse shows that the R.H.S is 15 % greater than the L.H.S. This discrepancy is due to the difficulty in estimating t_m and t_{ll} from the initial temperature distribution $T_{lb.m}(x,t)$ and $T_{l\,b.ev}(x_0,t_l)$.

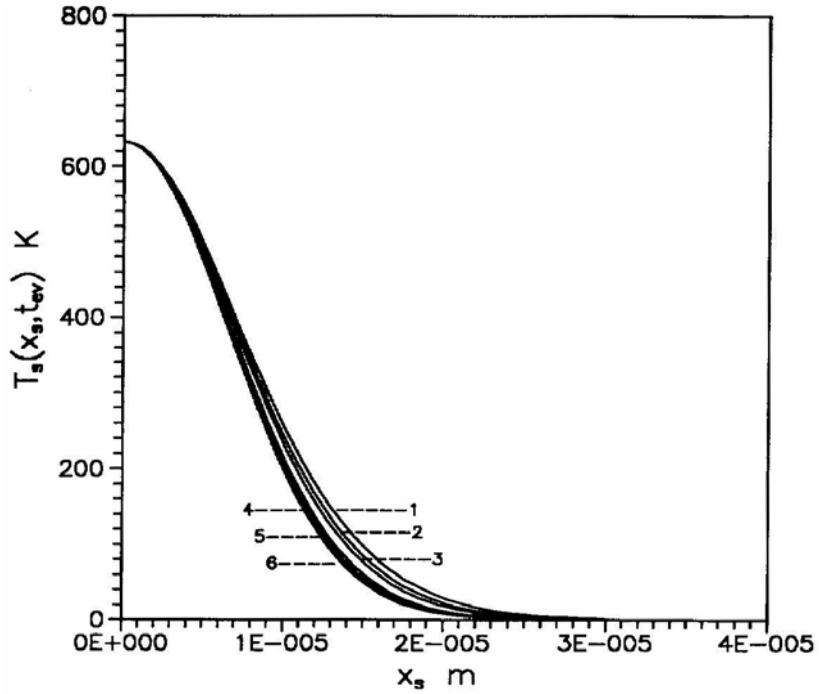

Fig.(5): The temperature distribution in the still solid part of an Al thin-film coated on a glass substrate irradiated with a Ready pulse profile of $\delta t = 2\times10^{-6}$s. The calculations were carried out for the cases listed in tables (3,4) at $t_{ev} = \left(\frac{\delta t - (t_m + t_{ll})}{10}\right)$ s after initiating the evaporation process and R=0.

Fig.(6) illustrates the temperature distribution within the substrate at $t_{ev} = [\delta t - (t_m + t_{ll})]$ for the same conditions given in Fig.(1). The figure shows, as expected, a drastically decay of the temperature within the substrate. This is due to the low thermal conductivity of the substrate's material. The penetration depth for $A_{01} = 3.05\times10^{-5}$ K^{-1} and $q_0 = 3.5\times10^{12}$ Wm^{-2} is greater than the case at which $A_{01} = 0$ K^{-1} and $q_0 = 2.5\times10^{12}$ Wm^{-2}. This is due to the greatest slope of the temperature in the solid part of the film at the substrate interface.

Figure (7) represents the time dependence of the evaporated thickness of the thin-film when q_0 is kept constant at 2×10^{12} Wm^{-2} and δt was varied according to tables (5) and (6). The figure shows as in Fig.(1) that by increasing δt the evaporated thickness increases and that at the end of the laser pulse the evaporated thickness for the case $A_{01} = 3.05\times10^{-5}$ K^{-1} (increased absorption) is about 3 times greater than that for $A_{01} = 0$ K^{-1}.

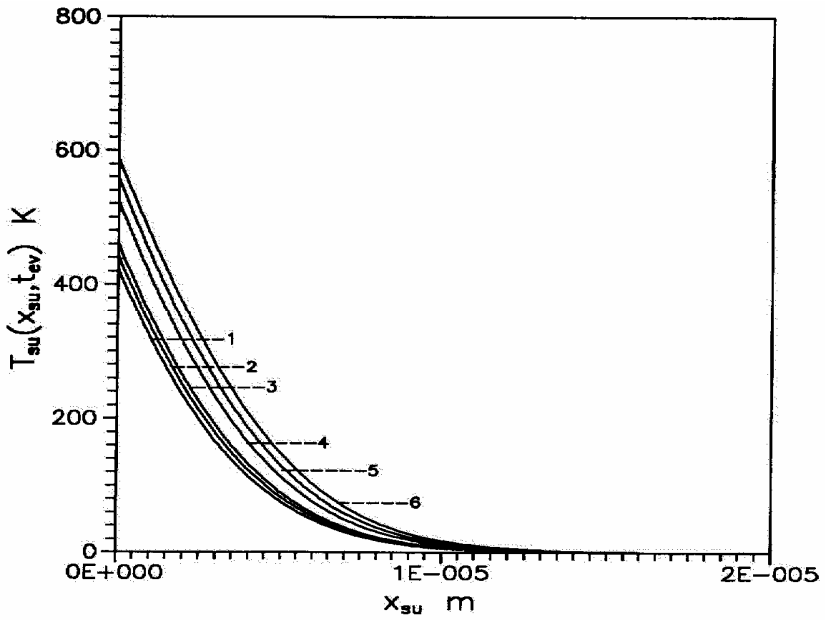

Fig.(6): The temperature distribution in a glass substrate coated with an Al-thin film and irradiated with a Ready pulse profile of $\delta t = 2\times10^{-6}$ s. The calculations were carried out for the cases listed in tables (3,4) at $t_{ev} = (\delta t - (t_m + t_{ll}))$ s after initiating the evaporation process and R=0.

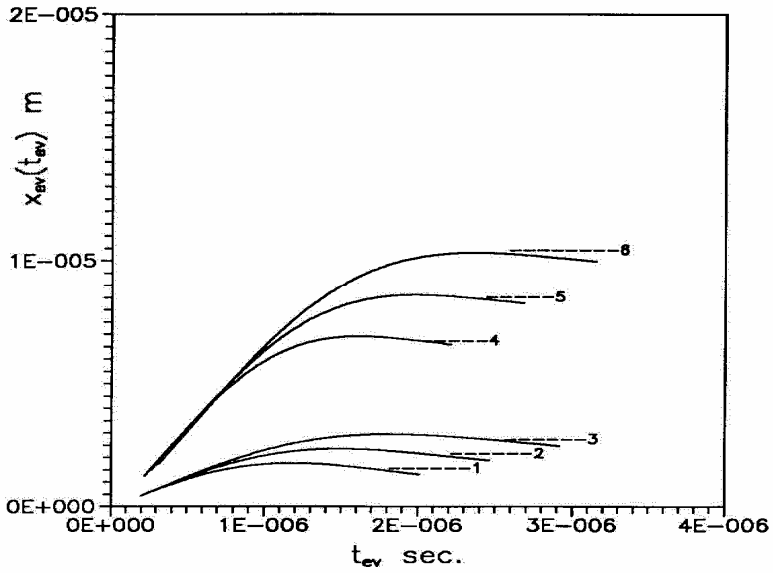

Fig.(7): The time dependence of the evaporated thickness $x_{ev}(t_{ev})$ calculated during the irradiation of an Al thin-film coated on a glass substrate with a Ready pulse profile of $q_0 = 2.0\times10^{12}$ Wm^{-2} .The calculations were carried out considering the cases listed in tables (5,6) and R=0.

Table (5): The values of the melting time t_m, the time of initiating the evaporation process t_{ll} and calculated for different values of δt ; $q_0 = 2 \times 10^{12}$ Wm^{-2}; $A_{01}=0$ K^{-1} and $L= 4\times10^{-5}$ m.

δt s	t_m s	t_{ll} s	curve no
2.5×10^{-6}	1.6300×10^{-7}	3.2880×10^{-7}	1
3.0×10^{-6}	1.8300×10^{-7}	3.5560×10^{-7}	2
3.5×10^{-6}	2.0173×10^{-7}	3.8180×10^{-7}	3

Table (6): The values of the melting time t_m, the time of initiating the evaporation process t_{ll} and calculated for different values of δt ; $q_0 = 2 \times 10^{12}$ Wm^{-2}; $A_{01}=3.05\times10^{-5}$ K^{-1} and $L= 4\times10^{-5}$ m.

δt s	t_m s	t_{ll} s	curve no
2.5×10^{-6}	1.4100×10^{-7}	1.4290×10^{-7}	4
3.0×10^{-6}	1.5700×10^{-7}	1.5950×10^{-7}	5
3.5×10^{-6}	1.7295×10^{-7}	1.7410×10^{-7}	6

Due to the existence of vapor, liquid and solid at any instant of time during the considered pulse duration in this work, the behavior of the obtained results shows that the effect of the substrate is limited.

Taking into account the same conditions given in Fig.(7), the calculations of the molten layer thickness as a function of time and the temperature distribution in the molten layer thickness , the still solid part of the thin-film and in the substrate show the same behavior as that in Figs. 2,2,4,5,6 respectively.

3.2. Case when the chemical reaction in the vapor is considered (R=1)

As the exothermic chemical reaction in the vapor was considered in the calculation, the evaporated thickness calculated at the same conditions of Fig.(1), was increased by about 20 %. Figure (8) shows the obtained results.

The time dependence of the evaporated thickness as well as the molten layer thickness, the temperature distribution in the liquid and the solid part of the thin-film, show the same behavior as in the case when no chemical reaction was considered, but with a slight decrease in the molten layer thickness and the penetration depth of the temperature distribution in the solid part of the target. This behavior is due to the increased evaporated part of the target.

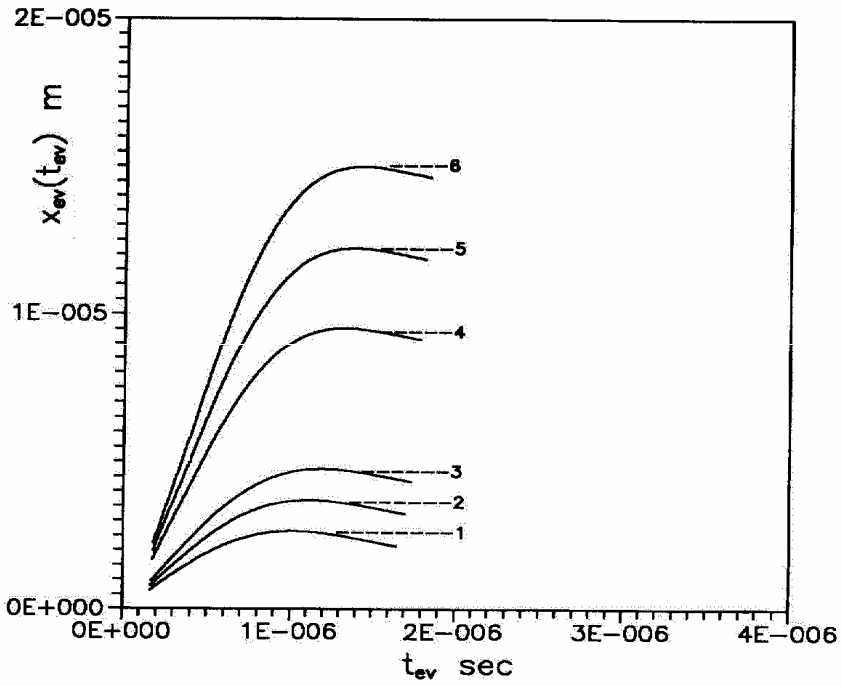

Fig.(8): The time dependence of the evaporated thickness $x_{ev}(t_{ev})$ calculated during the irradiation of an Al thin-film coated on a glass substrate with a Ready pulse profile of $\delta t = 2\times10^{-6}$ s. The calculations were carried out considering the cases listed in tables (3,4) and R=1.

4. Conclusions:

1. The formulas for the spatial and temporal temperature distributions in the molten layer thickness, the solid part of the thin film of the target and the substrate were obtained.
2. The molten layer thickness and the evaporated thickness can be determined by knowing the laser power of the incident pulse, the pulse duration of the target.
3. By increasing both of the power density and the pulse duration, the molten layer thickness and the evaporated thickness increases.
4. The chemical reaction plays an important role in increasing the evaporation process.
5. The substrate becomes more effective for small thin-film thickness.

References

1. J.F. Ready, "*Effects of high power laser radiation*" Academic Press, New York (1971).
2. E.M. Breinan, B.H. Kear and C.M.Banas, *Phys. Today* **29**, 44 (1967).
3. S.S. Charaschan, "*Lasers industry*" Van Nostrand, New York (1972) chap.4 and 5.
4. F.E. Haper and M.I. Cohen, *Solid-State Electron* **11**, 1176 (1968).
5. J.F. Ready, *J. Appl. Phys*. **36**, 462 (1965).
6. B.P. Fairand, B.A. Wilcox, W.J. Gallagher and D.N. Williams, *J. Appl. Phys*. **43**, 3893 (1972).
7. R.A. Ghez and R.A. Laff, *J. Appl. Phys*. **46**, 2103 (1975).
8. R.E. Warren and M. Sparks, *J. Appl. Phys*. **50**, 7952 (1979).
9. M. Sparks and E. Loh, *J. Opt. Soc. Am* **69**, 847 (1979).
10. A. Bhattacharyya and B.G. Streetman, *J. Phys. D:Appl.Phys*. **14**, L67 (1981).
11. D.L. Balageas, J.C. Krapez and P. Cielo, *J. Appl. Phys*. **59**, 348 (1986).
12. M.K. El-Adawi and E.F. El-Shahawey, *J. Appl. Phys*. **60**, 2250 (1986).
13. M.K. El-Adawi and S.A. Shalaby, *J. Appl. Phys*. **63**, 2212 (1988).
14. A.F. Hassan, M.M. El-Nicklawy, M.K. El-Adawi and A.A. Hemida, *Optics and Laser Technology* **25 (3),** 155 (1993).
15. S.E.-S. Abd El-Ghany, Ph.D. Thesis, Faculty of Science, Benha University, Egypt, (1998).
16. A.F. Hassan, M.M. El-Nicklawy, M.K. El-Adawi, E.M. Nasr, A.A. Hemida and O.A. El-Gaffar, *Optics and Laser Technology* **28 (5)**, 337 (1996).
17. M.M. El-Nicklawy, A.F. Hassan and S.E.-S. Abd El-Ghany, *Optics and Laser Technology* **32**, 157 (2000).
18. S.E.-S. Abd El-Ghany, *Optics and Laser Technology* **33**, 539 (2001).
19. S.E.-S. Abd El-Ghany, *Optics and Laser Technology* **26**, 95 (2004).
20. R. David Lide Editor in chief, "*Handbook of Chemistry and Physics*" 73 RD edition, CRC press Inc.(London), (1993).